

Forming pressure effect on microstructure and mechanical properties of nanocrystalline aluminum synthesized by inert gas condensation

Shangshu Wu, Zhou Yu, Junjie Wang, Hanxin Zhang, Chaoqun Pei, Shu Fu, Hao Fu, Jiajie Meng and Tao Feng*

Herbert Gleiter Institute of Nanoscience, Nanjing University of Science & Technology, Nanjing, People's Republic of China

Abstract. The preparation of nanocrystalline aluminum (NC Al) was conducted in two steps. After the NC Al powder was synthesized by an Inert gas condensation (IGC) method in a helium atmosphere of 500 Pa, the NC Al powder was in-situ compacted into a pellet with a 10 mm diameter and 250 μm -300 μm thickness in a high vacuum (10^{-6} Pa- 10^{-7} Pa) at room temperature. The NC Al samples were not exposed to air during the entire process. After the pressure reached 6 GPa, the relative density could reach 99.83%. The results showed that the grain size decreased with the increased of in-situ forming pressure. The NC Al samples present obvious ductile fracture, and the tensile properties were greatly changed with the increase of forming pressure.

1 Introduction

Aluminum and aluminum alloys play an important role in the aerospace and automotive industries owing to the excellent property, light in weight and resistant to corrosion. Therefore, research on aluminum has important practical significance[1]. The motivation for research interest in bulk nanostructured materials attributed to the excellent work of H.Gleiter and his Partners in the early 1980s. They first prepared bulk nanostructured materials by inert gas condensation (IGC) and found that their microstructure and properties are considerable different from traditional coarse-grained materials[2-4]. While changing the structure of the material, the strength as well as hardness of the material are improved[5, 6]. For nanocrystalline materials, a large number of interfacial structures can be introduced by reducing the size of the crystal grains to the nanometer magnitude. Due to the different arrangement of atoms at the interface and inside the grain, they show different properties[7]. The relevant properties of the material can be tuned by the introduced interface defect. A recent study by F. Tang and cooperators[8] explained the deformation mechanism of thin film nanocrystalline aluminum (NC Al) prepared under different vacuum degrees. The variation of interfacial oxygen content is used as a variate to explain the effect of impurities on the mechanical properties and thermal stability of NC Al. The performance is proportional to the oxygen content, which is also suitable for thermal stability. M. Abou Zied et al. found that effect of peaks expansion at different pressures on the structure of nanocrystals in XRD test[9]. Under different pressures, the lattice constant of the sample shows a regular change, and the pressure has a

significant influence on the internal microstructure of the NC Al. High grain size stability of NC Al was introduced by F. Zhou. J. Lee found the thermal stability of NC Al of different grain sizes[10]. The thermal stability of NC Al can reach 0.78Tm. X. Z. Liao et al[5,11] showed the wide stacking faults formation mechanism and deformation twins in NC Al, a more profound explanation of the microscopic deformation mechanism of NC Al has been made. The grain size plays a crucial role in understanding the deformation mechanism of NC Al.

The preparation process of the material determines the microstructure of the sample, which affects the properties of the material. It is well known that the current methods for preparing bulk nanomaterials can be roughly divided into two categories: bottom-up and top-down. The inert gas condensation method is a typical bottom-up method, which structurally reorganizes metal materials from the atomic dimension, and is the most advantageous method for obtaining bulk nanomaterials at the current. In addition, the nanocrystalline material prepared by the inert gas condensation method is no longer limited to the thin film, and is more favorable for the study of the structure and properties of the bulk nanocrystalline materials.

In this work, NC Al was prepared by IGC method, and the in-situ forming pressure effect on the microstructure and mechanical properties of the NC Al was systematically studied. Under ultra-high pressure, the porosity of NC Al was reduced dramatically, and the density could reach 99.83% of the coarse grain Al. The microstructure of NC Al with different forming pressure were characterized by XRD, SEM, and TEM, and the mechanical properties were studied by the tensile test.

* Corresponding author: tao.feng@njust.edu.cn

2 Experimental procedure

The raw material was a commercially pure Al powder (purity \geq 99.9%), which was purchased from Ningbo Shanshan New Material Technology Co., Ltd. The NC Al was synthesized by an IGC method. As shown in the Fig. 1. (a) and (b), our IGC system consists mainly of three units, powder preparation unit, low pressure compaction unit, and high pressure compaction unit. At the first step, in the powder preparation unit, the raw material Al was evaporated in the helium (500 Pa) when the temperature reached 1400°C. Al atoms lost kinetic energy and condensed in the form of small crystals a few nanometers across, which accumulate on a vertical cold finger as a loose powder. The NC Al powder was stripped off and collected into a container. At the second step, the NC Al powder was transferred to the low pressure compaction unit and compressed into a pellet with 10 mm diameter under the pressure of 500 MPa. Finally, the pellet was transferred to the high pressure compaction unit to condense under the pressure of 2-6 GPa. Our NC Al sample is formed by pressure only, without any heat treatment.

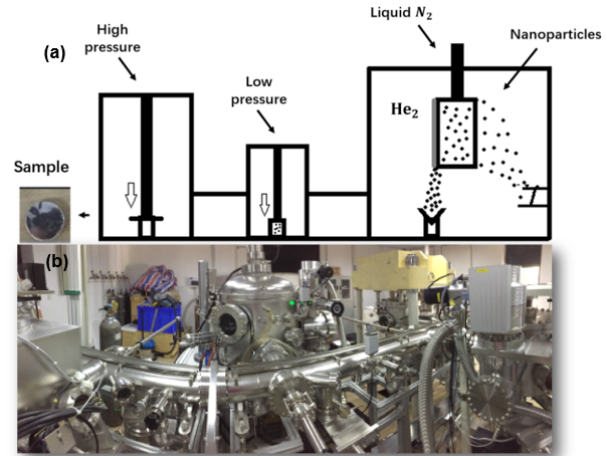


Figure 1. (a) the schematic diagram and (b) the photo of inert gas condensation (IGC) system.

The grain size of the NC Al powder and bulk NC Al sample were determined by X-ray diffraction (XRD) analysis and transmission electron microscope (TEM) observation. The XRD testing was carried out on a Bruker-AXS D8 Advance diffractometer with Cu K α radiation. Microstructures were characterized by a FEI Tecnai 20 (TECNAI G2 20 LaB6) transmission electron microscopy. The TEM powder specimen was prepared by dispersing NC Al powder in alcohol and dripping onto the TEM copper grid after ultrasounding for 20 min. The TEM foils specimen was prepared by mechanically polishing the NC Al pellet to the thickness of 50 μ m and then cutting into a circle with diameter of 3 mm, finally corroding in methanol mixed with nitric acid (7:3) solution. The density of NC Al samples was measured by volume-weight method (Archimedes principle). The tensile tests were conducted on instron E3000 tensile machine at room temperature, with a constant strain rate

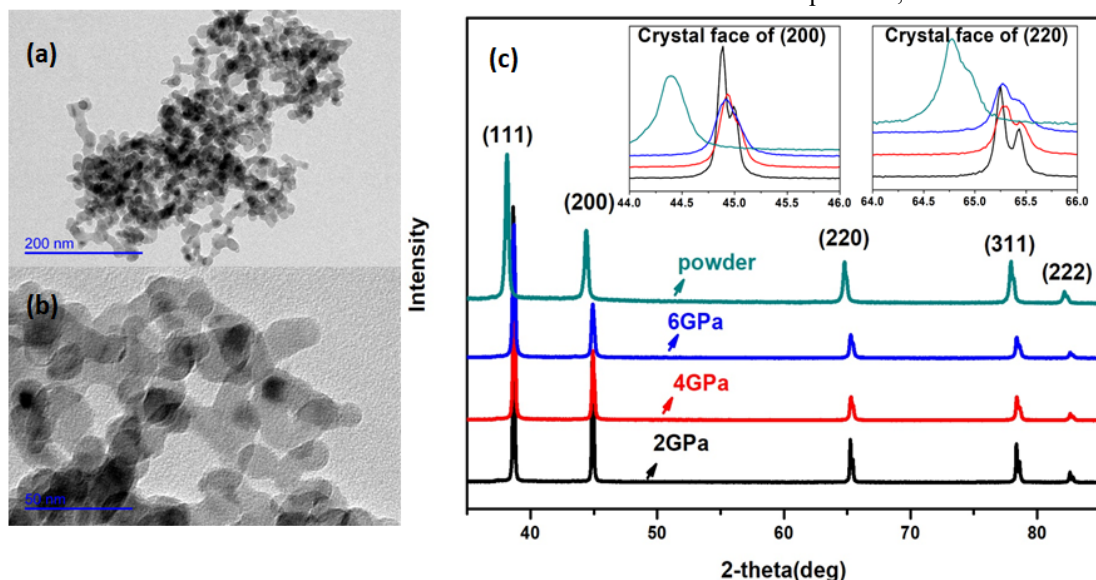


Figure 2. (a) and (b) are the TEM images of the as-prepared NC Al powder synthesized by inert gas condensation, (c) XRD patterns of NC Al powder and pellets under different forming pressure.

Table 1. Structural parameters under different pressures

sample	(200)/ θ°	(220)/ θ°	lattice constant / \AA	interplanar distance of (200) / \AA	interplanar distance of (220) / \AA
--------	-----------------------	-----------------------	---------------------------------	--	--

2GPa	44.882	65.247	4.04171	2.020855	1.42896
4GPa	44.886	65.256	4.04063	2.020315	1.42858
6GPa	44.909	65.263	4.0405	2.02025	1.42853

of $1 \times 10^{-4} \text{ s}^{-1}$. Crosshead displacement was used to calculate strain, the initial sample cross section was used to calculate stress, and the gage length after failure was used to calculate the elongation to failure of the sample.

The observation of the tensile-specimen fractures was made on a FEI Quanta 250F scanning electron microscope (SEM).

3 Results and discussion

Fig.2. (a) and (b) are the transmission electron micrograph of the NC Al powder. Dense alumina film appeared on the surface of the NC Al powder and prevented the further oxidation after the powder was taken out from the chamber. A statistical analysis of 500 grains showed an average particle size of 25 nm. The results of grain size tested by the TEM is consistent with the XRD calculation. Fig.2. (c) is a crystal plane diffraction peaks of NC Al. Firstly, the diffraction peaks of the two crystal faces of (200) and (220) are smoothly taken. The changes of the diffraction peak parameters under different forming pressures can be used to obtain the change of NC Al crystal structure after in-situ high

pressure compaction. The lattice constant is a basic parameter reflecting the structural size of the crystalline material, which directly reflects the binding energy between the particles. The magnitude of the change in lattice constant is small (about 10^{-5} nm). The lattice constant a can be calculated using the Bragg equation and the interplanar spacing formula. NC Al belongs to the face-centered cubic:

$$2 \sin \theta = n\lambda \quad (1)$$

$$a = \frac{\lambda}{2 \sin \theta} \sqrt{h^2 + k^2 + l^2} \quad (2)$$

Where, λ is the incident X-ray wavelength; n is the diffraction order; θ is the Bragg angle. The deviation in the measurement of the lattice constant is mainly derived from the wavelength λ , $\sin \theta$ and the interference surface index (h, k, l). n is usually taken as 1, λ is 0.154056 nm, and h, k, l are integers, so the source of the lattice constant deviation is mainly $\sin \theta$. The lattice constant can be obtained by bringing the parameters of Table 1 into the above formula. Bringing the obtained lattice constant into the formula of the interplanar spacing of the cubic crystal system, the interplanar spacing can be

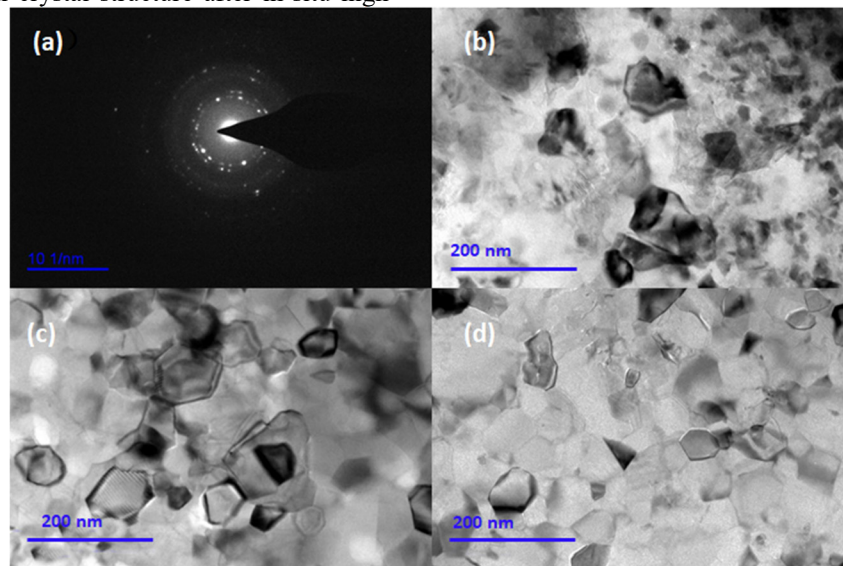


Figure 3. (a) diffraction pattern of 4 GPa NC Al, and TEM images of (b) 2 GPa, (c) 4 GPa, and (d) 6 GPa NC Al obtained.

$$d = \frac{a}{\sqrt{h^2 + k^2 + l^2}} \quad (3)$$

From the above results, it can be seen that as the in-situ pressure increases from 2 GPa to 6 GPa, the lattice constant decreases from 4.04171 Å to 4.04063 Å and then decreases to 4.0405 Å. It is owing to vacancies' formation[12]. It is also accompanied by a decrease in the interplanar spacing. The variation of the interplanar spacing is reduced from 2.020855Å of the (200) crystal plane to 2.02025Å, and the (220) crystal plane is reduced from 1.42896Å to 1.42853Å.

In addition, the influence of pressure on the grain size change can also be analyzed from the X-ray diffraction pattern. The larger the full width at half maximum (half width) of the diffraction peak on the diffraction curve,

the smaller the grain size. The grain size of the constituent material can be expressed by the full width at half maximum in the X-ray diffraction region. From the Fig. 2. (c) can be seen that as the molding in-situ pressure increases, significant peak broadening occurs, peak broadening and grain size closely related. Use the Scherrer formula can get the grain size:

$$D_{hkl} = \frac{0.89\lambda}{\beta \cos \theta} \quad (4)$$

Where, D_{hkl} is the grain size perpendicular to the (hkl) crystal plane; β is the half-height width of the diffraction peak due to microcrystal refinement. It can be seen from the measurement results that on the diffraction curve, the full width at half maximum of the (200) and (220) crystal plane diffraction peaks increased as the in-situ pressure increased. According to the Scherrer formula, with the

in-situ pressure increased, the grain size perpendicular to the (220) and (200) crystal planes gradually decreased.

Table 2. Grain size and density

sample/GPa	grain size/nm	density (g/cm ³)	Relative density
2GPa	94	2.3164	87.02%

4GPa	75	2.6325	98.89%
6GPa	45	2.6575	99.83%
raw material	/	2.662	100%
powder	26.7	/	/

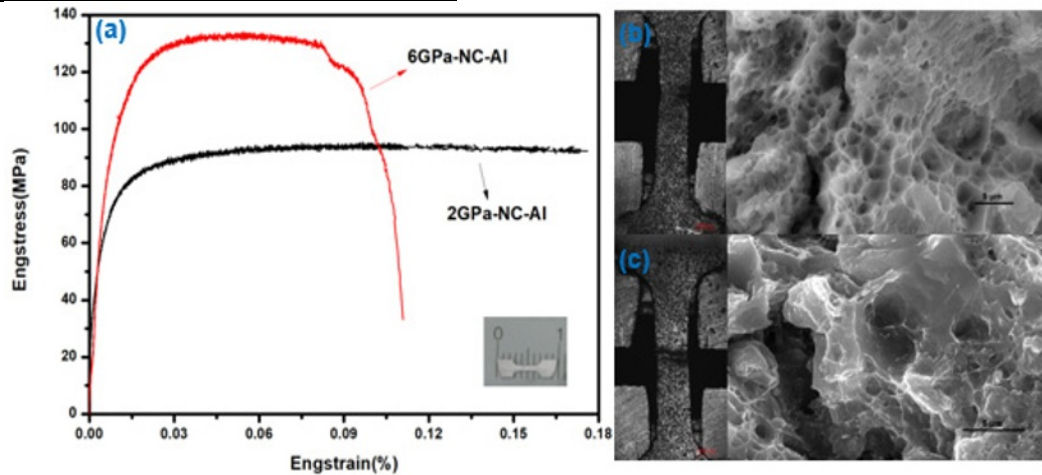


Figure 4. (a) tensile curve of 2 GPa and 6 GPa NC Al samples, (b) and (c) fractured surface of tensile specimens with 2 GPa and 6 GPa, respectively.

Sanders et al., [13] Ma., [14] and Youngdahl et al[15] have studied the effects of processing defects on nanocrystalline materials on mechanical properties. They showed the results that the processing defects would reduce hardness, strength, and plasticity. All of the processing defects may lead to untrustworthy information, mainly about mechanical properties. The current work also studies the effects of processing defects on the mechanical properties of samples. As the forming pressure increased from 2 GPa to 6 GPa, the grain size of the NC Al sample decreased from 94 nm to 45 nm. At the same time, the relative density of 6 GPa sample can reach 99.83% of coarse grain Al. Fig. 3. (a) is the diffraction pattern of 4GPa sample, it shows clear polycrystalline features. Fig. 3. (b) (c) and (d) show the grain size of NC Al, and it corresponds to the XRD result. Generally, the strength of polycrystals generally obeys the Hall-Petch relationship as the grain size changes[16].

$$\sigma = \sigma_0 + kd^{-1/2} \quad (5)$$

σ_0 is the intensity constant; k is the normal number; d is the grain size. According to the Hall-Petch empirical formula, the strength of the material is inversely related to the grain size of the material. For traditional coarse crystals, the deformation mechanism is the interaction of unit dislocations and the work hardening control plasticity. For nanocrystals, as the grain size decreases to the nanometer level, a large number of interfaces are introduced to produce high-density grain boundaries. Grain boundaries hinder the dislocation movement which causes the increasement of hardness and strength of the material. The deformation mechanism of the material becomes that dislocations and dislocation stacks emit from grain boundaries and promote grain boundaries to shear. However, when the grain size of the material is less than 10 nm, grain boundary sliding and grain rotation become the dominant deformation mechanism,

and an abnormal Hall-Petch relationship occurs[17-24].

As shown in the Fig. 4. (a), comparing the tensile properties of the NC Al samples under the forming pressure of 2 GPa and 6 GPa, the obtained results are consistent with the Hall-Petch relationship. The tensile strength of the NC Al increased from 94 MPa of 2 GPa samples to 134 MPa of 6 GPa samples, which is 40% increasement. The necking phenomena were observed during the tensile test for both kinds of NC Al. Fig. 4. (b) and (c) are the SEM photographs of the fractures of the two samples with a large number of dimples, which shows the obvious ductile fracture feature.

4 Conclusions

In this work, pure NC Al was prepared by IGC method under different in-situ forming pressure from 2 GPa to 6 GPa. The microstructure and mechanical preoperties were systematically studied by XRD, SEM, TEM and tensile test. When the pressure reached 6GPa, the relative density of the NC Al sample could reach 99.83%. With the forming pressure increase, the lattice constant and crystal surface spacing of the samples showed regular changes. The grain size decreased from 94nm to 45nm, and the tensile strength increased from 94 MPa. The tensile strength of 6 GPa sample increased by 40% comparing to 2 GPa sample. All the NC Al samples showed obvious ductile fracture.

Acknowledgment

This work was supported by the National Natural Science Foundation of China (grant no. 51571119) and the Fundamental Research Funds for the Central Universities (No. 30916011106). TF acknowledges the support by the innovation project, Qing Lan project and

the specially-appointed professor project of Jiangsu province.

References

1. I. Matsui, S. Ono, Y. Takigawa, T. Uesugi, K. Higashi. *Mater. Sci. Eng. A* **550**, 363 (2012)
2. H. Gleiter. *Prog. Mater. Sci* **33**, 223 (1989)
3. R. Birringer, H. Gleiter, H.P. Klein. *Phys. Lett. A* **41**, 1033 (1993)
4. H. Gleiter, P. Marquardt, *Z. Metallkunde* **75**, 263 (1984)
5. X.Z. Liao, F. Zhou, E.J. Lavernia. *Appl. Phys. Letters* **83**, 5062 (2003)
6. M.A. Meyers, A. Misher, D.J. Benson. *Prog. Mater. Sci* **51**, 427 (2006)
7. P.L. Sun, E.K. Cerreta, J.F. Bingert, G.T. Gray. *Mater. Sci. Eng. A* **464**, 343 (2007)
8. F. Tang, D.S. Gianola, M.P. Moody, K.J. Hemker, J.M. Cairney. *Acta. Mater* **60**, 1038 (2012)
9. M.A. Zied, A.A Ebnalwaled. *Intermetallics* **16**, 745 (2008)
10. F. Zhou, J. Lee. *J Mater Res* **16**, 12 (2001)
11. X.Z. Liao, S.G. Srinivasan, Y.H. Zhao, M.I. Baskes, Y.T. Zhu, F. Zhou, et al. *Appl. Phys. Letters* **84**, 3564 (2004)
12. R.A. Varin, J. Bystrzycki, A. Calka. *Intermetallics* **7**, 917 (1999)
13. P.G. Sanders, C.J. Youngdahl, J.R. Weertman. *Mater. Sci. Eng* **234**, 77 (1997)
14. L. He, E. Ma. *J. Mater. Res* **11**, 72 (1996)
15. C.J. Youngdahl, P.G. Sanders, J.A. Eastman, J.R. Weertman. *Scripta. Mater* **37**, 809 (1997)
16. G.D. Hughes, S.D. Smith, C.S. Pande. *Scripta. Metall. Mater* **20**, 93 (1986)
17. C.Y. Yu, P.W. Kao, C.P. Chang. *Acta. Mater* **53**, 4019 (2005)
18. H. Gleiter. *Adv Mater* **4**, 474 (1992)
19. S. Cheng, E. Ma, Y.M. Wang, et al. *Acta. Mater* **53**, 1521 (2005)
20. Y.M. Wang, E. Ma. *Acta. Mater* **52**, 1699 (2004)
21. H. Conrad, *Mater. Sci. Eng. A* **341**, 216 (2003)
22. K.S. Kumar, H.Van. Swygenhoven. S. Suresh. *Acta. Mater* **51**, 5743 (2003)
23. E.O. Hall. *Proc. Soc. London* **64**, 747 (1951)
24. N.J. Petch. *Iron Steel Inst* **174**, 51 (2006)